Monograph:
Coca, D., Balikhin, M. and Billings, S.A. (1999) Time-Domain Identification of Nonlinear Processes in Space Plasma Turbulence Using Multi-Point Measurements. Research Report. ACSE Research Report 760 . Department of Automatic Control and Systems Engineering

TIME-DOMAIN IDENTIFICATION OF NONLINEAR PROCESSES IN SPACE PLASMA TURBULENCE USING MULTI-POINT MEASUREMENTS

D. COCA[1], M. BALIKHIN[1], S.A. BILLINGS[1], H.St.C.K. ALLEYNE[1]

M. DUNLOP[2], H. LÜHR[3]

[1]ACSE, University of Sheffield, Sheffield, UK
[2] Imperial College, London, UK
[3] Geoforschungszentrum Potsdam, Germany

Department of Automatic Control and Systems Engineering,
University of Sheffield
Sheffield, S1 3JD,
UK

RESEARCH REPORT NO. 760
September 1999

TIME-DOMAIN IDENTIFICATION OF NONLINEAR PROCESSES IN SPACE PLASMA TURBULENCE USING MULTI-POINT MEASUREMENTS.

D. Coca[1], M.Balikhin[1], S.A. Billings[1] H. St. C. K. Alleyne[1], M. Dunlop[2], H. Lühr[3]

[1]ACSE, Sheffield University, Sheffield, S1 3JD, UK
[2] Imperial College, London, UK
[3] Geoforschungszentrum Potsdam, Germany

ABSTRACT

Nonlinear process identification techniques in the time-domain are adopted in the study of space plasma turbulence using multi-satellite measurements. These techniques are applied to the analysis of two point measurements from AMPTE UKS-AMPTE IRM in the terrestrial foreshock to identify the dynamical features in the turbulence, which could not be determined using a frequency domain approach previously applied to the same data.

Key words: nonlinear processes; plasma turbulence; nonlinear interaction.

1. INTRODUCTION

Identification of linear and nonlinear processes in the observed space plasma turbulence is an important task for the Cluster WEC community. The nonlinear process identification methods used so far in this area, such as Fourier modelling and high order spectral estimations, are based on frequency domain analysis of the data. In order to ensure reliable identification, spectral methods often require very long data sets, in particular when identification of cubic effects which arise in four wave processes, is needed. An alternative approach is to perform system identification in the time domain. One of the most powerful methods for time-domain, nonlinear system identification is based on the NARMAX (Nonlinear AutoRegressive Moving Average with eXogenous inputs) model introduced by Leontaritis and Billings (1985).

This study presents the first application (to our knowledge) of nonlinear system identification techniques based on the NARMAX model, in the identification of nonlinear processes in space plasma turbulence. The measurements of magnetic turbulence obtained by AMPTE UKS-AMPTE IRM in the vicinity of the quasi-parallel part of the terrestrial bow shock, are used to estimate a discrete-time nonlinear model. It is shown that the identified model can accurately predict the magnetic field measured by AMPTE-IRM, the output of the model, based only on the observations made by AMPTE UKS, regarded as the input of the model.

2. BRIEF COMPARISON WITH THE DIRECT TRANSFER FUNCTION ESTIMATION APPROACH

The existing approaches to determining the Generalised Frequency Response Functions, using multidimensional spectrum estimation, have several drawbacks. These include the great computational burden and the difficulties associated with the implementation of multi-dimensional Fast Fourier Transforms and multidimensional windowing/smoothing. In addition, the amount of data required to obtain reasonable estimates, the number of parameters required to represent the higher order spectra, which increases geometrically with the order of the nonlinear frequency response function, and the assumptions regarding the number of terms in the series are all limiting factors. As a result, in practice it is often assumed that only the first and second order Volterra kernels exist and that these can be estimated with sufficient accuracy using the data available. Unfortunately, the truncation of the Volterra expansion to only two terms is in many cases not sufficient to fully capture the underlying nonlinear interactions in the data. The four-wave interactions in particular are very important in the study of turbulence, so it is essential to be able to model these types of processes accurately.

This task can be successfully accomplished by using nonlinear system identification techniques to estimate a mathematical model of the process in the time domain. The method proposed here to study plasma turbulence involves the identification of a NARMAX model from two-point satellite measurements. In practice, this requires only a relatively small estimation data set and involves the estimation of a very small number of model parameters, compared with the direct frequency domain identification method.

The main advantage of this approach is that the model can then be used to analyse the nonlinear processes in a plasma both in the time and frequency domain. This can be achieved by analytically mapping the identified time-domain NARMAX model into the

frequency domain. The NARMAX model can therefore be used to compute the nonlinear frequency response functions up to any desired order without any assumptions regarding the number of terms in the series. The analytical form of the frequency response functions also makes it possible to analyse in detail any particular frequency range and to study which time domain model terms induced these effects.

Despite the much smaller parameter set, the NARMAX model can provide an excellent approximation to the entire underlying nonlinear process that is modelled, hence it should be possible to study two-four-wave and theoretically even higher interactions.

3. NONLINEAR SYSTEM IDENTIFICATION USING THE NARMAX METHOD

The only available information regarding a nonlinear system is often in the form of a discrete set of input and output observations $u^N = (u(1), ... u(N))$ and $y^N = (y(1), ... y(N))$. Determining the function or mathematical model which describes the causal input/output dependence, that is the input/output behaviour of a system, is of paramount importance in system theory.

NARMAX is a parameter estimation methodology for estimating both the structure and the parameters of the unknown nonlinear system from the input/output data alone. The NARMAX model provides a concise mathematical representation of the observed discrete-time input/output behaviour, by relating explicitly the sampled output signals of the system to the sampled inputs applied to the system. The class of behaviours that can be represented using NARMAX models is extremely large and includes many other nonlinear model classes, such as the Volterra, Hammerstein and Wiener models, as special cases.

The NARMAX model takes the form of a set of nonlinear difference equations, one for every output of the system. It should be noted that the identification methodology applied here for a Single-Input Single-Output (SISO) system, works equally well for Multi-Input Multi-Output (MIMO) systems.

The general form of the NARMAX model can be written as

$$\begin{aligned} y(t) \;=\; & F[y(t-1), ... y(t-n_y), \\ & u(t-1), ..., u(t-n_u), \\ & e(t-1), ..., e(t-n_e)] + e(t) \end{aligned} \qquad (1)$$

where $F : \mathcal{Y}^{n_y} \times \mathcal{U}^{n_u} \times \Xi^{n_e} \rightarrow \mathcal{Y}$ is the unknown multi-valued nonlinear function, $u(t) \in \mathcal{U}$ and $y(t) \in \mathcal{Y}$ are the input and the output vectors belonging to the m- and l-dimensional vector spaces $\mathcal{U}$ and $\mathcal{Y}$ respectively, $e(t) \in \Xi$ is a vector of unobserved stochastic variables, assumed bounded and uncorrelated with the input, n_u, n_y and n_e are the maximum input, output and noise lag.

Unlike in linear system identification, where knowledge of the model order is sufficient to define the model and estimate the parameters, when the system is nonlinear, the tasks involved are far more complex.

The black box system identification method based on the NARMAX model, requires solving the coupled problems of selecting the structure and estimating the parameters for the unknown nonlinear function F.

Because of the immense number of possible combinations, the difficulty involved in determining the form and parameters of F is considerable. This difficult problem is usually addressed using non-parametric regression techniques. More precisely, F is expanded in terms of a finite set of known (basis) functions or regressors belonging to given function class $\mathcal{F}$. Typical regressor classes include polynomial or rational functions, neural networks or wavelets.

The polynomial implementation was used in this study since it provides a simple and convenient model representation particularly suitable for both time- and frequency domain analyses. For polynomial models, equation (1) takes the form of a linear expansion in the polynomial terms g_k

$$y_i(t) = \sum_k \theta_k^i g_k^i(t) + e_i(t) \qquad (2)$$

The selection of the model terms was performed using the Orthogonal Forward Regression (OFR) algorithm. This least-squares based algorithm involves a stepwise orthogonalisation of the regressors and a forward selection of the relevant terms in (2) based on the Error Reduction Ratio (ERR) criterion. The algorithm also provides the optimum least-squares estimate of the corresponding parameter vector $\Theta = \{\theta_k\}$.

4. DESCRIPTION OF THE EXPERIMENT.

The data used in this study were collected by the AMPTE (Active Magnetospheric Particle Tracer Explorers) satellites UKS (United Kingdom Subsatellite) and IRM (Ion Release Module) on the day 30-10-1984. The data sets came from the magnetometer instruments on board each spacecraft. The UKS fluxgate magnetometer (PI D. J. Southwood) [Southwood et al., 1985] was a modified version of the ISEE 1/2 instrument. The IRM fluxgate magnetometer (PI H. Lühr) was described in [Lühr et al., 1985].

The crossing of the quasi-parallel shock on that day was intensively studied. In particular, modelling in the frequency domain was applied to the identification of linear and nonlinear processes in the magnetic field turbulence observed during that crossing [Dudok de Wit, 1999].

5. BRIEF DESCRIPTION OF THE RESULTS OF PREVIOUS STUDIES OF TURBULENCE OBSERVED DURING THE CROSSING OF QUASI-PARALLEL SHOCK ON 30.10.1984.

The plasma turbulence in the vicinity of the quasi-parallel part of the front of the terrestrial bow shock

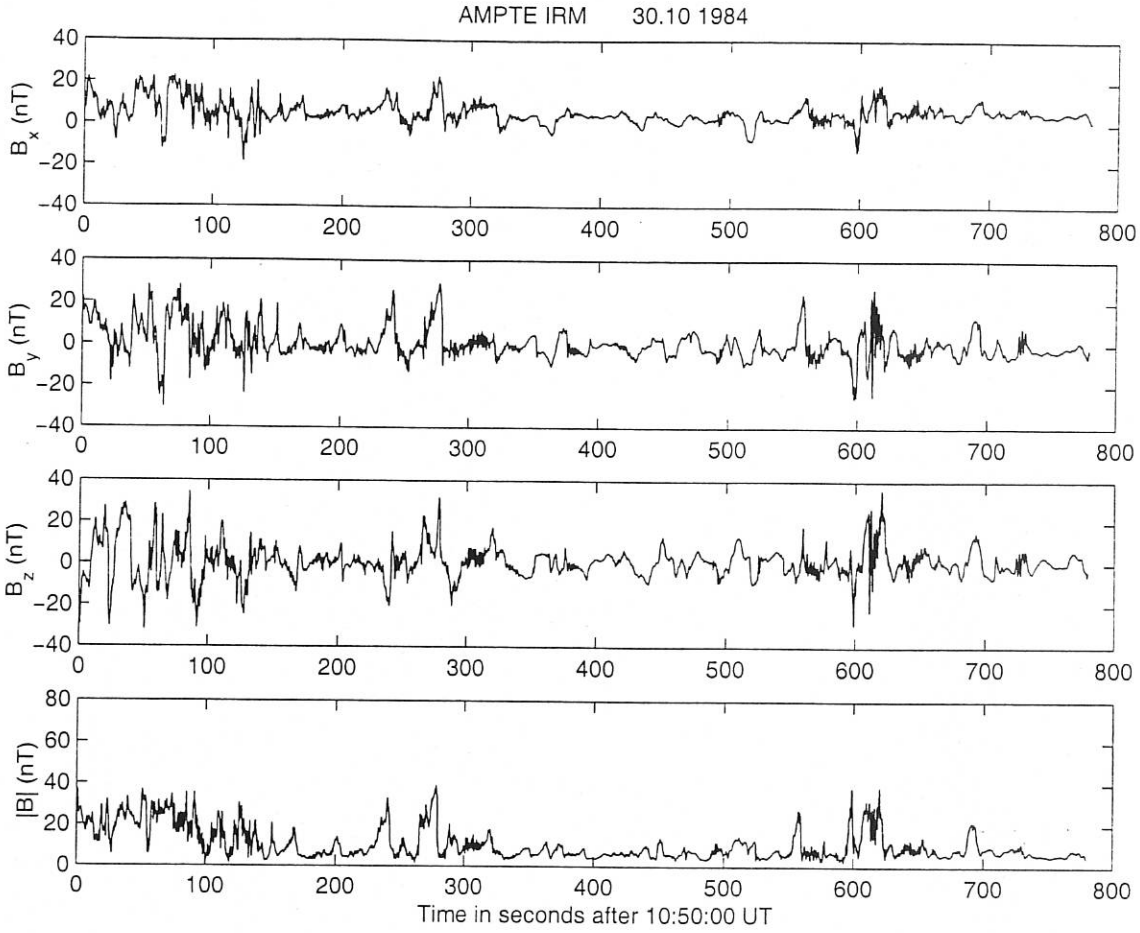

Figure 1. The magnitude and three GSE components of the magnetic field measured by AMPTE IRM during the period on 30.10.1984. Time in seconds after 10:50:00 UT

attracts considerable interest in various studies because it is rich with wave phenomena and various linear and nonlinear processes including such fundamental processes as steepening of nonlinear waves and generation of wave trains.

Different populations of ions reflected from the shock are related to various low frequency waves. Other electro-magnetic phenomena include Hot Flow Anomalies (also referred to as Active Current Sheets or Hot Diamagnetic cavities) which are characterised by a region of hot plasma whose bulk flow deviates considerably from anti-sunward solar wind flow [e.g. Schwartz, 1991]. Schwartz et al., [1988]. and Schwartz, [1991] divided nonlinear wave phenomena observed in the vicinity of the front of the quasi-parallel shock into two types. The first type includes structures "nested" relative to the shock. Nested structures often are regarded as short bow shock encounters. The other type includes structures "convected" with the solar wind. The other classification proposed by them subdivides wave structures into relatively short ($\approx$ 10 *seconds*) isolated or identifiable single excursions of the magnetic field (Short Large Amplitude Magnetic Structures. "SLAMS") and longer periods of enhanced, turbulent field "Long Pulsations" (LPs). Often SLAMS are observed to be embedded into Long Pulsations. Schwartz et al., [1988], and Schwartz. [1991] showed that while LPs often show a nested signature all SLAMS observed by them including those embedded in LPs are convected with the flow. LPs usually have a higher value of β. SLAMS grow from a ULF wavefield. Wave trains often are observed to be attached to SLAMS. Some models attribute primary significance to the SLAMS in the formation of the shock front. Schwartz and Burgess [1991] concluded that the front of a quasi-parallel shock could be considered as a superposition of SLAMS. which gradually decelerate the solar wind and lead to the formation of the downstream state.

The magnitude and three components (GSE) of the magnetic field as measured by AMPTE IRM on 30.10.1984 in the vicinity of the quasi-parallel shock are plotted in Figure 1. A few SLAMS (e.g. at 550 seconds past 10:50:00 UT) can be seen on this figure. A part of long pulsation has been observed at the beginning of interval (until 140 seconds).

6. IDENTIFICATION AND VALIDATION OF THE NONLINEAR MODEL

As convected waves were first encountered by AMPTE UKS and then by AMPTE IRM, the data set measured by AMPTE UKS and by AMPTE IRM

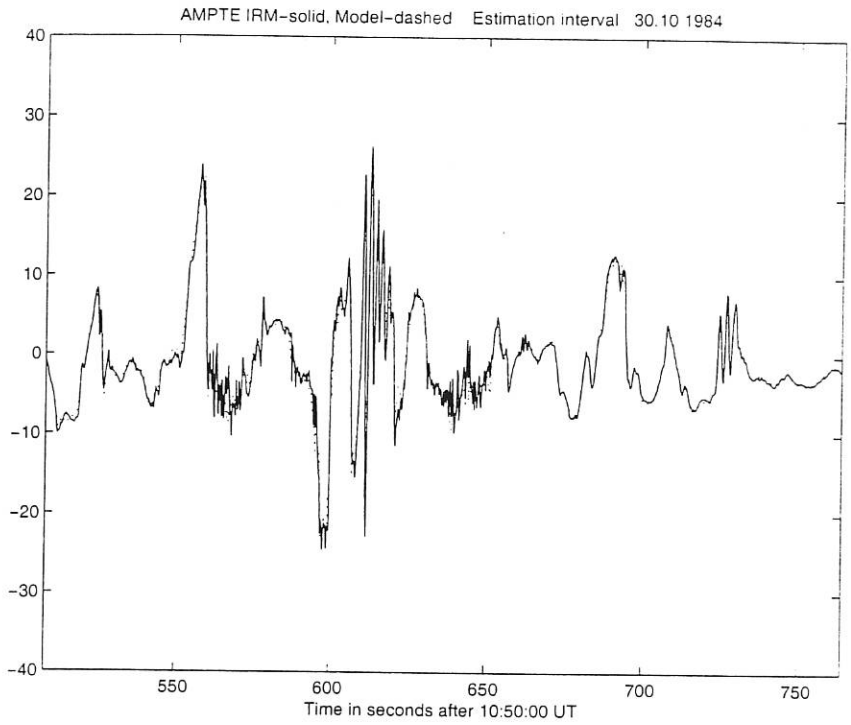

Figure 2. The B_y GSE components of the magnetic field measured by AMPTE IRM (solid line) and the output of the derived time domain model (dotted line) for the time interval which was used to identify the model. Time in seconds after 10:50:00 UT on 30.10.1984.

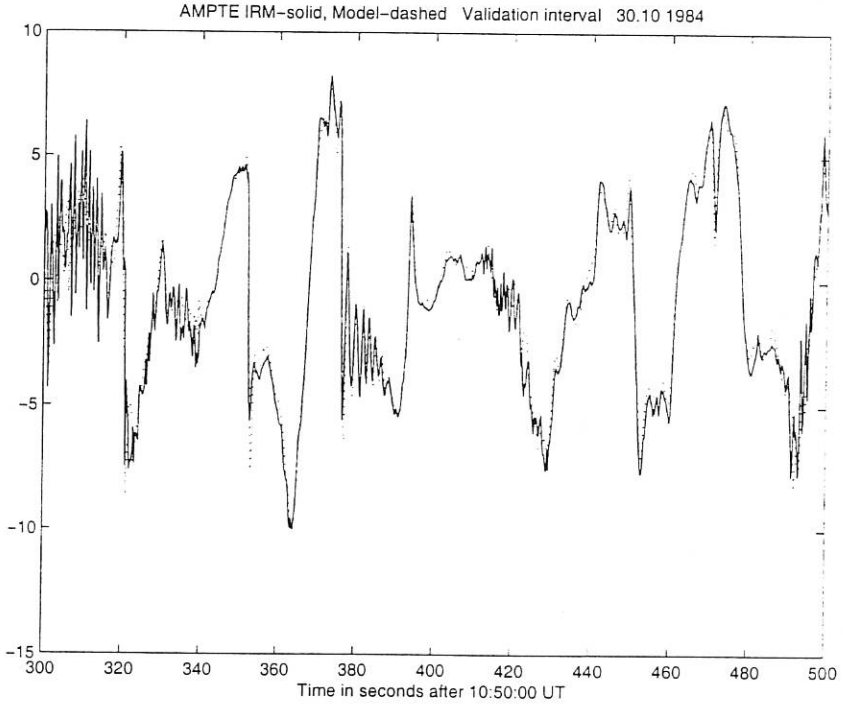

Figure 3. The B_y component (GSE) of the magnetic field measured by AMPTE IRM (solid line) and output of the derived time domain model (dotted line) the validation time interval which was not used in the identification of the model. Time in seconds after 10:50:00 UT on 30.10.1984.

were considered as the input and output of the system, respectively. 1000 pairs of input/output data points from 525 seconds were used in identification. The nonlinear model was identified using data corre-

sponding the the B_y component of the magnetic field only.

The remaining data was reserved for validating the nonlinear model. If the hypothesis that the model has generated the data (i.e. both the estimation data and the data reserved for validation) is true, then the model should be able to predict well the dynamics in both situations. The comparison between the real AMPTE IRM measurements of B_y used in estimation (solid line) and the output generated by the identified model (dotted line) is presented in Figure 2.

The model was also validated using the data set not used in estimation. The comparison between the model output and the real data is presented in Figure 3. This shows that the model predicts very well the magnetic field fluctuations measured by AMPTE IRM.

The visual evaluation of the model predictions does not illustrate how the model performs over a particular frequency range. This is shown by performing coherency analysis. More precisely the calculation of the coherency function

$$\gamma(f) = \frac{\langle B_{y\ pred} B^*_{y\ real} \rangle}{\langle |B^2_{y\ pred}| \rangle \langle |B^2_{y\ real}| \rangle}$$

provides insight into the relationship between $B_{y\ pred}$ and $B_{y\ real}$, the spectral components at the frequency f of the predicted and real data sets respectively. $\langle \cdot \rangle$ denotes averaging. The value of the coherency is bounded between 0 and 1. A value of coherency close to 1 means high correlation between the spectral components of the two data sets. A value close to zero means complete independence between two signals at that particular frequency. The magnitude and phase of the coherency function calculated for the real measurements and the output of the model are plotted in Figure 4a.b.

The coherency estimated from a finite point data set is a statistical value, the distribution of which is related to the real value of the coherency between the two signals. In particular the variance of the phase is determined by the real value of the coherency. It can be seen that coherency is very high (> 0.9) up to the frequency 0.6 Hz, i.e. in the frequency range which contains most of the energy of the turbulence. That frequency range contains both SLAMS for which the frequency is usually less than $0.1 - 0.2$ Hz, and important ULF waves such as for example whistler wave trains or shocklets which are observed usually in the frequency range $0.2 \geq f \geq 0.5$ Hz. At the same time the value of the phase is distributed around 0 for the same frequency range implying the absence of an artificial delay in the derived model. As we mentioned above the same interval of data was used in [Dudok de Wit et al., 1999] for identification of the nonlinear processes using modelling in the frequency domain. Dudok de Wit et al., [1999] also used the coherency function to validate their model. Although their coherency function is relative high for low frequencies, which correspond to SLAMS $f < 0.2$ Hz, it is very low < 0.35 for the frequencies which correspond to whistler wave trains. Such a low coherency implies that their model does not describe the dynamics of this second class of waves well. On the contrary high coherency of our time-domain models provides confidence that this model represents well the dynamics of both SLAMS, whistler packets and possible energy transition between them

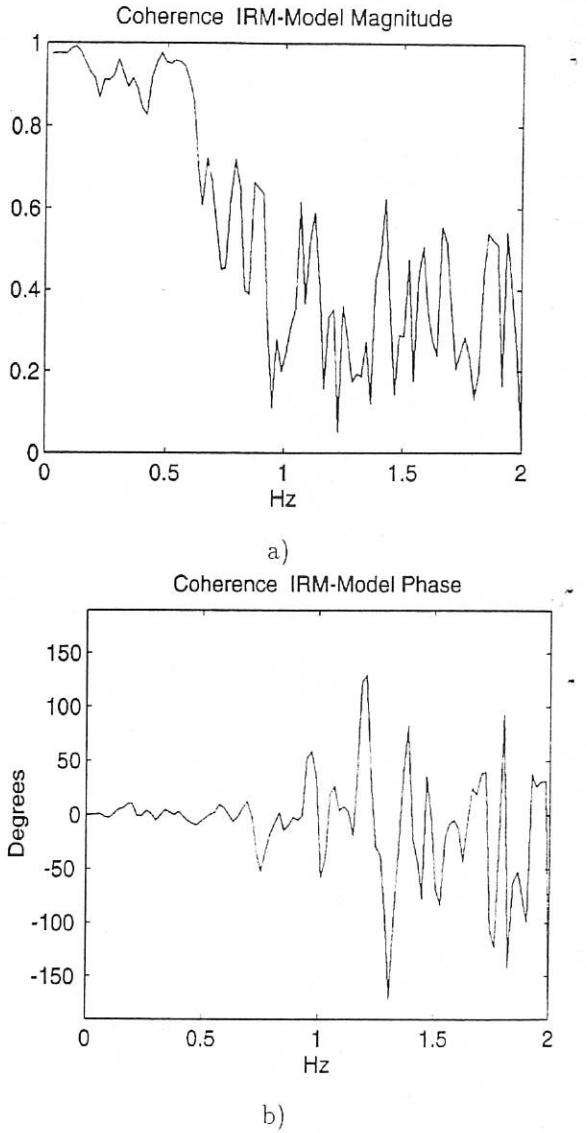

Figure 4. The magnitude and the phase of the coherency function calculated for the B_y component (GSE) of the magnetic field measured by AMPTE IRM and output of the derived time domain model.

7. ANALYSIS AND INTERPRETATION OF THE MODEL

Because the NARMAX identification procedure produced a particularly simple model form, which does not include any delayed output terms in the structure such that

$$y(t) = F(u(t-1), \ldots, u(t-n_u)) \qquad (3)$$

and the fact that F was identified as a cubic linear-in-the-parameters polynomial model, allows the dynamics of the system to be expressed as a superposition of three types of interactions

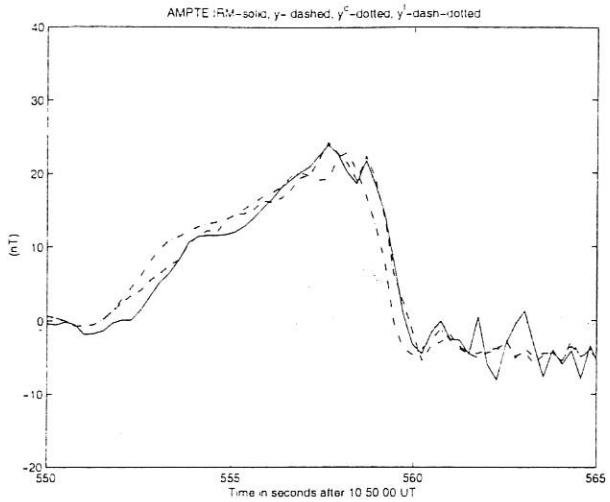

Figure 5. The B_y component (GSE) of the magnetic field measured by AMPTE IRM (solid line), output of the derived time domain model (dashed line), output of the linear (dashed-dotted line) and cubic (dotted line) parts of the model derived for the SLAMS observed at 555-565 seconds. Time in seconds after 10:50:00 UT on 30.10.1984.

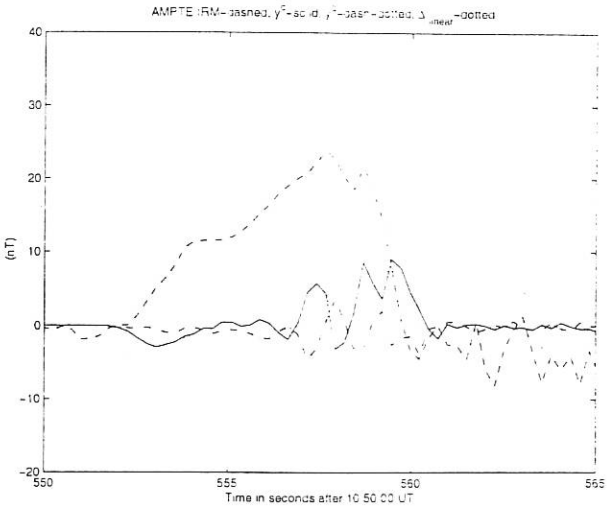

Figure 6. The B_y component (GSE) of the magnetic field measured by AMPTE IRM (dashed line) , cubic part of the model derived (solid line), quadratic part of the model derived (dashed-dotted line) and a difference between real data and the output of the linear part of the model (Δ_{linear}) as (dotted line).for the SLAMS observed at 555-565 seconds. The same time period as in Figure 4. Time in seconds after 10:50:00 UT on 30.10.1984.

$$\begin{aligned} y(t) &= y^l(t) + y^q(t) + y^c(t) \\ &= F^l(u(t-1)...) + F^q(u(t-1)....) + \\ &\quad F^c(u(t-1),...) \end{aligned} \quad (4)$$

where F^l, F^q and F^c denote the submodels involving only linear, quadratic and cubic polynomial terms respectively.

This decomposition approach was used to analyse in more detail the structure and interactions involved in the generation of one of the SLAMS measured by AMPTE IRM. The measured SLAM (solid line), superimposed with the model output (dashed line) and with the linear (dashed-dotted) and the cubic (dotted) output components y^l and y^c are plotted in Figure 5. Similar to Figure 2 it shows a good agreement between the real output and the model predicted output. It can also be seen that the linear part of the model provides a relatively good representation of the dynamics of the system. The cubic contribution is negligible except in the regions where the magnetic field gradient is significant. The real measurements of the same SLAMS (dashed), and the cubic contribution to the model (solid line) are also plotted in Figure 6 together with the quadratic contribution (dashed-dotted line) and the difference between the real data and the output of the linear part of the model Δ_{linear} (dotted line). Two further conclusions can be drawn from Figure 6. The first one is that for the dynamics the quadratic contribution is less important than the cubic. It can also be seen from Figure 6 that significant cubic contribution almost coincides with Δ_{linear}. Summarising, the dynamics of SLAMS and lower amplitude ULF waves appears to be linear except in their interface region where the cubic nonlinearity becomes important.

Similar conclusions can be drawn by considering any other SLAMS in our data (excluding those which are embedded in LP). The importance of nonlinearity at the SLAMS boundary regions is a manifestation of the fundamental process of steepening of a finite amplitude wave due to the nonlinearity (usually it is a simple hydrodynamic nonlinearity). The dynamics of SLAMS and the majority of ULF waves observed during the data interval under investigation, is mainly linear (outside the boundaries of SLAMSs). However a single exception was found in which the nonlinear part of the model plays a very important role through the whole structure. This exception is shown in Figures 7-9.

The measurements recorded by AMPTE IRM (solid line), the output of the identified model y (dashed line) and the output y^l generated by the linear part of the model (dotted line) are plotted in Figure 6. There are two wave events observed during that interval. One of these is a SLAMS observed during time interval 604-610 seconds. Its dynamics is similar to that described above (See Figures 5 and 6). However for the second event a large amplitude wave packet shows different dynamics. While the model provides a good representation of the evolution of real measurements for that wave packet, there is an obvious phase shift between the real data and the linear part of the model output. The real measurements of the AMPTE IRM for the same time interval (solid line), the output of the linear part of the model (dotted line) and output of the cubic part of the model (dashed-dotted line) are plotted in Figure 7. It can be seen that cubic part "corrects" the phase of the linear part of the model.

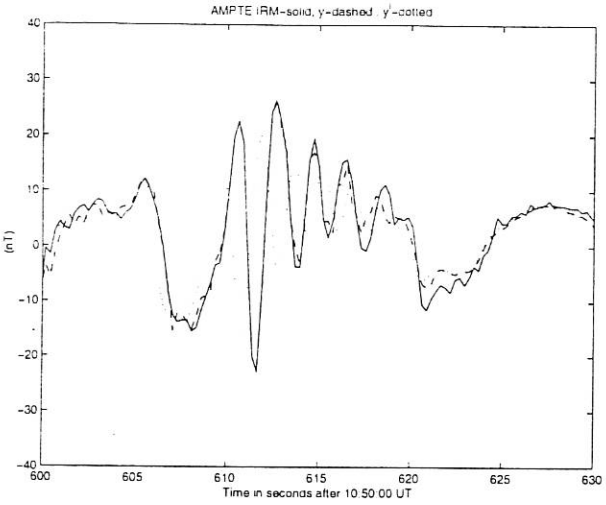

Figure 7. The B_y component (GSE) of the magnetic field measured by AMPTE IRM (solid line), the output of the derived nonlinear time domain model (dashed line), the output of the linear part of the model (dotted line) for the SLAMS observed at 604-610 seconds and nonlinear wave packet at 610-621 seconds. Time in seconds after 10:50:00 UT on 30.10.1984.

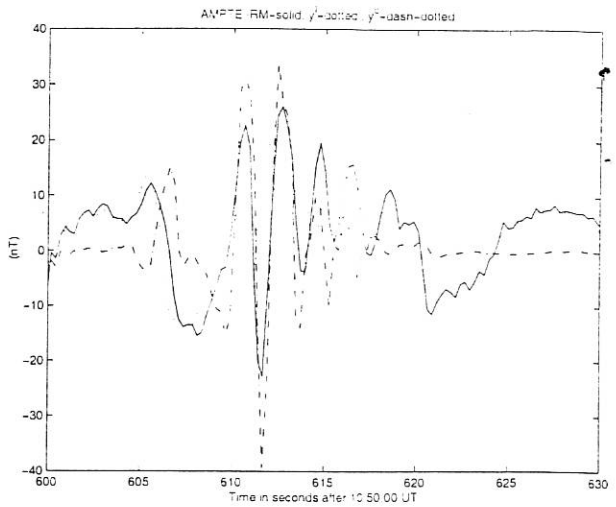

Figure 8. The B_y GSE components of the magnetic field measured by AMPTE IRM (solid line), output of the linear part (dotted line) of the model and output of the cubic part of the model (dashed-dotted line) for the SLAMS observed at 604-610 seconds and nonlinear wave packet at 610-621 seconds. The same time period as in Figure 6. Time in seconds after 10:50:00 UT on 30.10.1984.

This is even more obvious in Figure 8, where the real measurements are superimposed with the cubic component y^c of the model output and the linear model error Δ_{linear} (dotted line). In this case the cubic nonlinearity has a significant role in changing the phase velocity of the wave.

These effects are well known in theory. Mjolhus and Wyller (1986) for example, have shown that quasi-parallel, circularly polarised MHD waves of finite amplitude obey the Derivative Nonlinear Schröedinger (DNLS) equation :

$$\frac{\partial b}{\partial t} + \alpha \frac{\partial b}{\partial x}\left(|b|^2 b\right) + i\beta \frac{\partial^2 b}{\partial x^2} = 0$$

Where α and β are some parameters. The solution of this equation takes the form:

$$b = A_0 exp i\left(kx - \omega t\right)$$

where $\omega = \alpha A_0^2 k - \beta k^2$. Thus the dependence of the phase velocity $V_{ph} = \frac{\omega}{k}$ with amplitude A_0 exists due to the cubic nonlinearity. Previously [Dudok De Wit et al., 1995] pointed out a similar effect as a possible explanation of differences between maxima in the joint frequency-wave number spectrum and joint frequency-wave probability density.

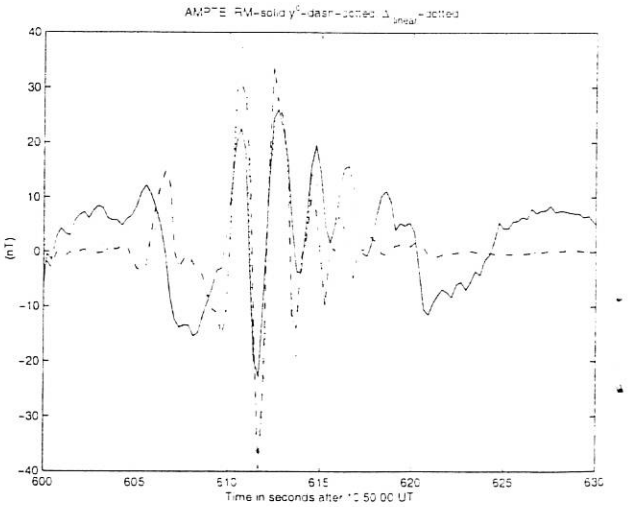

Figure 9. The B_y component (GSE) of the magnetic field measured by AMPTE IRM (solid line) , the output of the cubic part of the model (dashed-dotted line) and Δ_{linear} (dotted line) for the SLAMS observed at 604-610 seconds and nonlinear wave packet at 610-621 seconds. The same time period as in Figures 6 and 7 . Time in seconds after 10:50:00 UT on 30.10.1984.

To summarise, the analysis indicates that linear processes, such as propagation, linear growth due to the plasma instability or damping, make a significant contribution to the dynamics of both SLAMSs and ULF waves. Cubic nonlinearities are important at the boundaries of SLAMS, where they are responsible for steepening and energy transfer from SLAMS to the ULF waves. A single high amplitude wave packet was observed for which cubic nonlinearity made a very important contribution to the apparent phase velocity of the wave packet.

8. CONCLUSIONS

A time-domain identification approach based on the NARMAX model was applied in the identification and analysis of linear and nonlinear processes in space plasma turbulence. The main advantages of this method compared with the direct multi-spectrum estimation approaches previously adopted, are the relatively short amount of data required for estimation and the fact that the resulting NARMAX model appears to provide a far more accurate description of the dynamics with far less adjustable parameters than the low-order truncated Volterra expansions. This in turn means that it is easier to interogate the model and to relate the model terms to the underlying physical phenomena.

The NARMAX model identified from magnetic turbulence data obtained by AMPTE UKS - AMPTE IRM in the vicinity of the quasi-parallel part of the terrestrial bow shock, provides important insight into the fundamental nonlinear processes taking place in the plasma turbulence including wave steepening and nonlinear phase velocity shifts. Although these processes have been known from theory for a long time, until now there has not been much explicit experimental evidence of their importance in the dynamics of turbulence in space plasma .

9. BIBLIOGRAPHIC REFERENCES

REFERENCES

Dudok de Wit T., V.V. Krasnosel'skikh, S.D. Bale, M.W., Dunlop, H. Lühr, S.J. Schwartz and L.J.C. Woolliscroft, 1995. Geophys. Res. Lett, 22, 2653.

Dudok de Wit T., V.V. Krasnosel'skikh, M.W., Dunlop, H. Lühr, 1999, J. Geophys. Res., 104, 17079.

Dunlop, M. W., D. J. Southwood, K.-H. Glassmeir and F. M. Neubauer, 1988. Adv. Space Res., 8, (9)373.

Leontaritis, I.J., Billings, S.A., 1985. Int. J. Control. 41, (2)303.

Lühr, H.,N. Klöckler, W. Oelschägel, B. Häusler, and M. Acuna, 1985. The IEEE Trans. Geosci. and Remote Sensing GE-23, 259.

Mann G., H. Lühr, W. Baumjohann, 1994, J. Geophys. Res., 99, 13315.

Mjolhus E. and J. Wyller, Physica Scripta 1986, 33, 442.

Schwartz, S. J., 1991, Adv. Space Res., 11(9), 231.

Schwartz, S. J., And D. Burgess, 1991, Geophys. Res. Lett, 18, 373.

Schwartz, S. J., R. L. Kessel, C.C. Brinca, L.J.C. Woolliscroft, M. Dunlop , C.J. Farrugia and D.S. Hall, 1988, J. Geophys. Res., 93, 11295.

Southwood, D.J., W.A.C. Mier-Jedrzejowicz, and C.T. Russell, 1985, IEEE Trans. Geosci. and Remote Sensing GE-23, 301.